Bull. Chem. Soc. Jpn., **72**, 1285—1292 (1999)

Hydrophobic Interaction of *mer*-Tris(α-amino acidato)cobalt(III) with Tetrabutylammonium Ion

Yasuki Yoshimura

Laboratory of Chemistry, Faculty of Humanities and Social Sciences, Iwate University, Ueda, Morioka 020-8550

(Received January 13, 1999)

An interaction of NaBr, NH_4Br, Me_4NBr, Et_4NBr, Pr_4NBr, Bu_4NBr, and $NaBPh_4$ with *mer*-(+)-tris(L-alaninato)-cobalt(III) (*mer*-(+)-[Co(L-ala)$_3$]) was examined by estimating the standard enthalpy (ΔH°_{tr}) and entropy of transfer (ΔS°_{tr}) of *mer*-(+)-[Co(L-ala)$_3$] from water to the salt solutions on the basis of the temperature dependence of solubility. A difference in correlation between ΔH°_{tr} and $T\Delta S^\circ_{tr}$ demonstrated that while NaBr and NH_4NBr increase the solubility of *mer*-(+)-[Co(L-ala)$_3$] by hydrophilic interaction, Pr_4NBr, Bu_4NBr, and $NaBPh_4$ increase the solubility of *mer*-(+)-[Co(L-ala)$_3$] by hydrophobic interaction. On the basis of this finding, ΔH°_{tr} and $T\Delta S^\circ_{tr}$ of the transfer from water to aqueous Bu_4NBr solution for the *mer*-tris(aniono)cobalt(III) of glycine (glyH), L-alanine (alaH), L-serine (serH), DL-2-aminobutylic acid (abaH), DL-norvaline (nvalH), L-valine (valH), and L-leucine (leuH) led to the conclusion that hydrophobicity of the amino acids increases in the order of glyH < serH < alaH < abaH < nvalH < valH < leuH. This conclusion is compared with the hydrophobicity order reported in the literature.

As a model to clarify an interaction between proteins and water, various properties of amino acids[1—6] or small peptides[7—10] in aqueous solutions have been examined. In these approaches, a contribution of side chains of amino acids to the properties has become of interest. Amino acids exist mainly as zwitterions in aqueous solutions and the contribution of side chains is mostly estimated by subtracting the properties of glycine (glyH) from the properties of any amino acids.[2,5] But it has been suggested that an electrostatic interaction of the ionic end groups ($-NH_3^+$ and $-COO^-$) of the glyH zwitterion with water molecules is stronger than the interaction of other amino acids.[1,3] In addition, it is pointed out that the contribution of the ionic end groups to some properties of amino acids in aqueous solutions is much larger than the contribution of side chains.[2,6] Thus, since an interaction between side chains of amino acids and water molecules is strongly affected by the ionic end groups of their zwitterions, amino acids themselves are not necessarily adequate model compounds to examine the hydration of amino acid residues of proteins.

Nitta et al.[11,12] have investigated partial molar volumes and adiabatic compressibilities of *N*-acetyl-amino acid amides in dilute aqueous solutions from these standpoints and found that the influence of hydrogen bond formation of amide groups with water molecules on the hydration of side chains of these compounds is smaller than the influence of the electrostriction of the ionic end groups of the corresponding amino acid zwitterions.

I have investigated the dissolution behavior in water[13] and salt effects on the solubility[14,15] of tris(α-amino acidato)-cobalt(III) ([Co(aa)$_3$]). The amino acid in this chelate binds to the cobalt ion through both the amino nitrogen atom and the oxygen atom of the carboxylato group, and loses the amphotericity that causes the zwitterion formation. Thus, it would be expected that [Co(aa)$_3$] could be a suitable model compound for amino acid residues of proteins.

Tris(L-amino acidato)cobalt(III) has two geometric isomers (*mer*- and *fac*-isomers) and each geometric isomer has two diastereoisomers (Λ- and Δ-isomers). In this paper the Λ- and Δ-isomers are expressed as (+)- and (−)-isomers, which represent dextrorotatory and levorotatory at 589 nm, respectively. In general, the *mer*-isomer is more soluble than the *fac*-isomer and the (−)-isomer is more soluble than the (+)-isomer. The preceding investigation found that the moderately soluble *mer*-(+)-isomer is the most suitable isomer for an examination of solute–solvent interaction using the solubility measurement technique.[15]

As the first step to examine interactions between side chains of amino acids and water by using [Co(aa)$_3$] as the model compound, the solubilities of *mer*-(+)-tris(aniono)-cobalt(III) of various L-amino acids (*mer*-(+)-[Co(L-aa)$_3$]) in water and in aqueous solutions of hydrophobic salts such as tetraalkylammonium salts were measured over the temperature range of 5 to 40 °C. From these data, the standard enthalpy (ΔH°_{tr}) and entropy of transfer (ΔS°_{tr}) from water to the aqueous salt solutions for *mer*-(+)-[Co(L-aa)$_3$] were calculated. Since the tetraalkylammonium salts have been used to examine the strength of hydrophobic interactions,[16—19] it may be expected that ΔH°_{tr} and ΔS°_{tr} would give information on the hydrophobicity of amino acid side chains.

The hydrophobic interaction is one important factor that contributes to the folded conformation characteristic of proteins[20] and the hydrophobicity of amino acid side chains has been reported.[21] The validity of this approach in which *mer*-(+)-[Co(L-aa)$_3$] is used as the model compound for side chains of amino acid residues of proteins is discussed by comparing these estimates of the hydrophobicity with the reported one.

Experimental

The synthesis and separation of *mer*-(+)-[Co(L-aa)$_3$] of glyH, L-alanine (alaH), L-valine (valH), and L-leucine (leuH) were done in a manner similar to that reported in the literature.[22—24] These chelates are abbreviated as *mer*-[Co(gly)$_3$], *mer*-(+)-[Co(L-ala)$_3$], *mer*-(+)-[Co(L-val)$_3$], and *mer*-(+)-[Co(L-leu)$_3$], respectively. The separation of the diastereoisomers of *mer*-[Co(L-val)$_3$] and *mer*-[Co(L-leu)$_3$] was done by column chromatography on Florisil instead of the alumina reported in the above literature.

The separating ability of Florisil was superior to the ability of alumina. When *mer*-[Co(L-leu)$_3$] was eluted with 85% ethanol, the separation between the first and the second bands was satisfactory enough to isolate pure *mer*-(−)-[Co(L-leu)$_3$] by slowly evaporating the first eluent. The (+)-isomer was isolated by slow addition of water to the second eluent. But the separation of two bands was incomplete in the case of *mer*-[Co(L-val)$_3$]. The leading fractions from a number of preparations were collected and recromatographed once again, and pure fractions were carefully collected by monitoring the absorption spectrum of the eluent. The (−)-isomer was carefully crystallized by slow evaporation of these collections. When the trailing fractions from these preparations were concentrated to half, crude materials of the (+)-isomer were crystallized. The (+)-isomer could be purified by recrystallization from water. The absorption spectra of the chelates thus obtained agreed with the spectra reported in the literature.[24]

The less soluble isomers of *mer*-[Co(aa)$_3$] of DL-2-amino-butylic acid (abaH) and DL-norvaline (nvalH) were synthesized and separated in the same manner as those used for *mer*-(+)-[Co(L-val)$_3$]. Since the antipode of *mer*-(+)-[Co(L-aa)$_3$] is *mer*-(−)-[Co(D-aa)$_3$],[13b] the less soluble isomers of *mer*-[Co(DL-aba)$_3$] and *mer*-[Co(DL-nval)$_3$] are racemates, that is, equimolar mixtures of *mer*-(−)-[Co(D-aa)$_3$] and *mer*-(+)-[Co(L-aa)$_3$]. These isomers are abbreviated as *mer*-(−+)-[Co(DL-aba)$_3$] and *mer*-(−+)-[Co(DL-nval)$_3$], respectively. The spectroscopic properties and analytical data of these chelates are as follows: for *mer*-(−+)-[Co(DL-aba)$_3$]: ($\lambda_{\max}$/nm, $\varepsilon_{\max}$/(10 dm^2 mol^{-1})): (539, 105); (373, 161). Calcd for $Co(C_4H_8NO_2)_3\cdot 3H_2O$: C, 34.4; H, 7.2; N, 10.0%. Found: C, 34.3; H, 7.2; N, 10.1%. For *mer*-(−+)-[Co(DL-nval)$_3$]: ($\lambda_{\max}$/nm, $\varepsilon_{\max}$/(10 dm^2 mol^{-1})): (534, 105); (373, 163). Calcd for $Co(C_5H_{10}NO_2)_3\cdot 2H_2O$: C, 40.6; H, 7.7; N, 9.5%. Found: C, 40.2; H, 7.4; N, 9.5%.

The solubility in mol kg^{-1} (S_m), which was defined as the moles of chelate molecules in 1 kg of water or an aqueous salt mixture, and the solubility in mol dm^{-3} (S_c) at 25 °C were measured as previously reported.[13] The chelate concentration in saturated solution used to calculate the solubility was determined spectrophotometrically by measuring the absorbance at a wavelength in the vicinity of 530 to 540 nm, except for the experiment for *mer*-(+)-[Co(L-leu)$_3$] in water, in which the absorbance at 220 nm was measured because of low solubility of *mer*-(+)-[Co(L-leu)$_3$] in water. The solubility measurement was repeated at least four times at each temperature and the errors defined as the deviations at 95% confidence levels were less than 2% of the mean values of these individual experimental values in most cases.

Commercial ammonium bromide (NH_4Br), tetramethylammonium bromide (Me_4NBr), tetraethylammonium bromide (Et_4NBr), tetrapropylammonium bromide (Pr_4NBr), tetrabuthylammonium bromide (Bu_4NBr), and sodium tetraphenylborate ($NaBPh_4$) (reagent grade, Wako Chemical Industries Ltd.) were used without further purification. The working solution of each salt for the solubility measurement was prepared at 25 °C and the salt concentration was calculated in both mol kg^{-1} and mol dm^{-3} (m_s and c_s, respectively). Redistilled water was used.

Results and Discussion

Solubility, Standard Enthalpy, and Entropy of Dissolution of *mer*-(+)-[Co(L-aa)$_3$] in Water. The values for the solubilities (S_m° and S_c°) in water of *mer*-[Co(gly)$_3$], *mer*-(+)-[Co(L-ser)$_3$], *mer*-(−+)-[Co(DL-aba)$_3$], *mer*-(−+)-[Co(DL-nval)$_3$], *mer*-(+)-[Co(L-val)$_3$], and *mer*-(+)-[Co(L-leu)$_3$] are tabulated in Table 1. Since the solubilities of these chelates are fairly small, these saturated solutions may be regarded as being ideal dilute solutions with respect to the chelates. Thus, without an activity correction the standard enthalpy (ΔH_s°) and entropy of dissolution (ΔS_s°) in water at 25 °C were estimated from the temperature dependence of $\ln S_m^\circ$ illustrated in Fig. 1, where $\ln S_m^\circ$ is plotted against $1/T$, in the same manner as previously reported.[25] The standard state for the chelate in solution is 1 mol kg^{-1}.

The values for ΔH_s° and $T\Delta S_s^\circ$ of the adopted chelates in water at 25 °C are listed in Table 2, where the values of *mer*-(+)-[Co(L-ala)$_3$] estimated from the S_m° data obtained in the previous study[15] are also included. While both ΔH_s° and $T\Delta S_s^\circ$ of *mer*-[Co(gly)$_3$], *mer*-(+)-[Co(L-ala)$_3$], *mer*-(+)-[Co(L-ser)$_3$], and *mer*-(−+)-[Co(DL-aba)$_3$] are positive, ΔH_s° and $T\Delta S_s^\circ$ of *mer*-(−+)-[Co(DL-nval)$_3$], *mer*-(+)-[Co(L-val)$_3$], and *mer*-(+)-[Co(L-leu)$_3$] are negative. It is

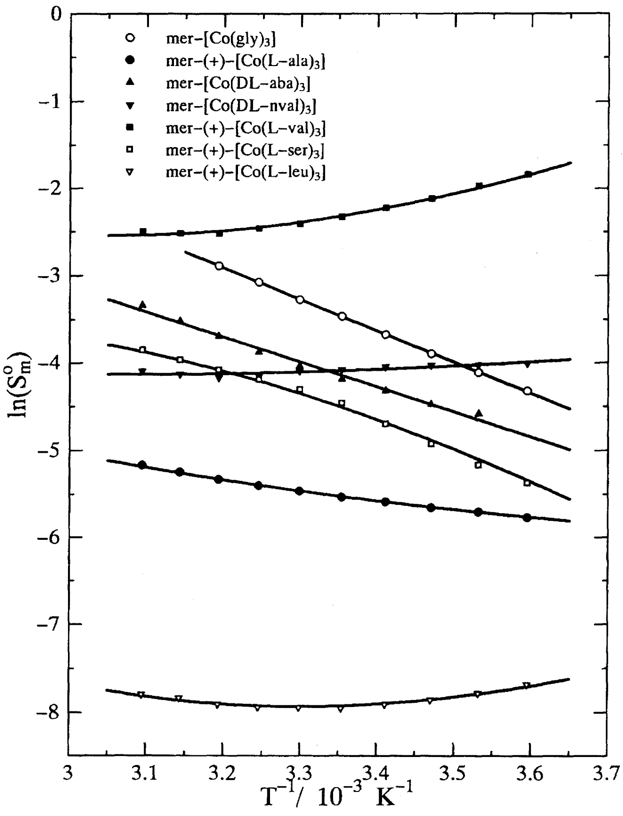

Fig. 1. Solubility curves of various *mer*-[Co(aa)$_3$] in water illustrated by plotting $\ln S_m^\circ$ against $1/T$.

Table 1. Solubilities (S_m° and S_c°) of *mer*-[Co(gly)$_3$], *mer*-(+)-[Co(L-ser)$_3$], *mer*-(−+)-[Co(DL-aba)$_3$], *mer*-(−+)-[Co(DL-nval)$_3$], *mer*-(+)-[Co(L-val)$_3$], and *mer*-(+)-[Co(L-leu)$_3$] in Water[a)]

T/°C	*mer*-[Co(gly)$_3$]	*mer*-(+)-[Co(L-ser)$_3$]	*mer*-(−+)-[Co(DL-aba)$_3$]	*mer*-(−+)-[Co(DL-nval)$_3$]	*mer*-(+)-[Co(L-val)$_3$]	*mer*-(+)-[Co(L-leu)$_3$]
	$S_m^\circ/10^{-2}$ mol kg^{-1}	$S_m^\circ/10^{-2}$ mol kg^{-1}	$S_m^\circ/10^{-2}$ mol kg^{-1}	$S_m^\circ/10^{-2}$ mol kg^{-1}	$S_m^\circ/10^{-1}$ mol kg^{-1}	$S_m^\circ/10^{-4}$ mol kg^{-1}
5	1.33(0.01)	0.467(0.003)		1.83(0.01)	1.59(0.01)	4.63(0.03)
10	1.64(0.02)	0.573(0.005)	1.02(0.01)	1.79(0.01)	1.39(0.01)	4.18(0.07)
15	2.04(0.02)	0.727(0.006)	1.14(0.01)	1.78(0.01)	1.20(0.01)	3.88(0.05)
20	2.54(0.04)	0.912(0.002)	1.33(0.01)	1.75(0.02)	1.08(0.01)	3.69(0.06)
25	3.14(0.01)	1.16(0.01)	1.52(0.01)	1.70(0.02)	0.974(0.006)	3.53(0.03)
30	3.78(0.01)	1.35(0.01)	1.77(0.01)	1.66(0.01)	0.897(0.009)	3.55(0.01)
35	4.63(0.01)	1.52(0.01)	2.08(0.01)	1.57(0.01)	0.851(0.004)	3.57(0.02)
40	5.56(0.05)	1.70(0.01)	2.49(0.02)	1.55(0.01)	0.801(0.007)	3.68(0.02)
45		1.90(0.02)	2.96(0.05)	1.61(0.02)	0.805(0.006)	3.96(0.06)
50		2.13(0.01)	3.55(0.04)	1.67(0.02)	0.822(0.008)	4.14(0.05)
	$S_c^\circ/10^{-2}$ mol dm^{-3}	$S_c^\circ/10^{-2}$ mol dm^{-3}	$S_c^\circ/10^{-2}$ mol dm^{-3}	$S_c^\circ/10^{-2}$ mol dm^{-3}	$S_c^\circ/10^{-1}$ mol dm^{-3}	$S_c^\circ/10^{-4}$ mol dm^{-3}
25	3.21(0.01)	1.18(0.01)	1.56(0.01)	1.74(0.02)	0.981(0.010)	3.62(0.02)

a) Errors defined as 95% confidence levels are given in parentheses.

Table 2. Standard Enthalpy (ΔH_s°) and Entropy of Dissolution (ΔS_s°) in Water at 25 °C for *mer*-[Co(gly)$_3$], *mer*-(+)-[Co(L-ala)$_3$], *mer*-(+)-[Co(L-ser)$_3$], *mer*-(−+)-[Co(DL-aba)$_3$], *mer*-(−+)-[Co(DL-nval)$_3$], *mer*-(+)-[Co(L-val)$_3$], and *mer*-(+)-[Co(L-leu)$_3$]

Compound	ΔH_s°/kJ mol^{-1}	$T\Delta S_s^\circ$/kJ mol^{-1}
mer-[Co(gly)$_3$]	29.8	21.2
mer-(+)-[Co(L-ala)$_3$][a)]	9.1	−4.6
mer-(+)-[Co(L-ser)$_3$]	26.1	15.0
mer-(−+)-[Co(DL-aba)$_3$]	22.1	11.7
mer-(−+)-[Co(DL-nval)$_3$]	−5.2	−15.3
mer-(+)-[Co(L-val)$_3$]	−13.7	−19.5
mer-(+)-[Co(L-leu)$_3$]	−2.6	−22.3

a) Calculated from the solubility data reported in Ref. 15.

interesting to compare the dissolution behavior of *mer*-[Co(aa)$_3$] in water with the behavior of *fac*-[Co(aa)$_3$]. The comparison will be reported elsewhere in connection with a difference in the solubilities of the diastereoisomers of *mer*-[Co(aa)$_3$].

Effects of Various Tetraalkylammonium Bromides and NaBPh$_4$ on the Solubility of *mer*-(+)-[Co(L-ala)$_3$]. The values for S_m and S_c of *mer*-(+)-[Co(L-ala)$_3$] in aqueous NH$_4$Br, Me$_4$NBr, Et$_4$NBr, Pr$_4$NBr, Bu$_4$NBr, and NaBPh$_4$ solutions are tabulated in Table 3. To demonstrate any change in the solubility caused by an addition of the salts, log (S_c°/S_c) is plotted against c_s in Fig. 2, where the effect of NaBr[15)] is

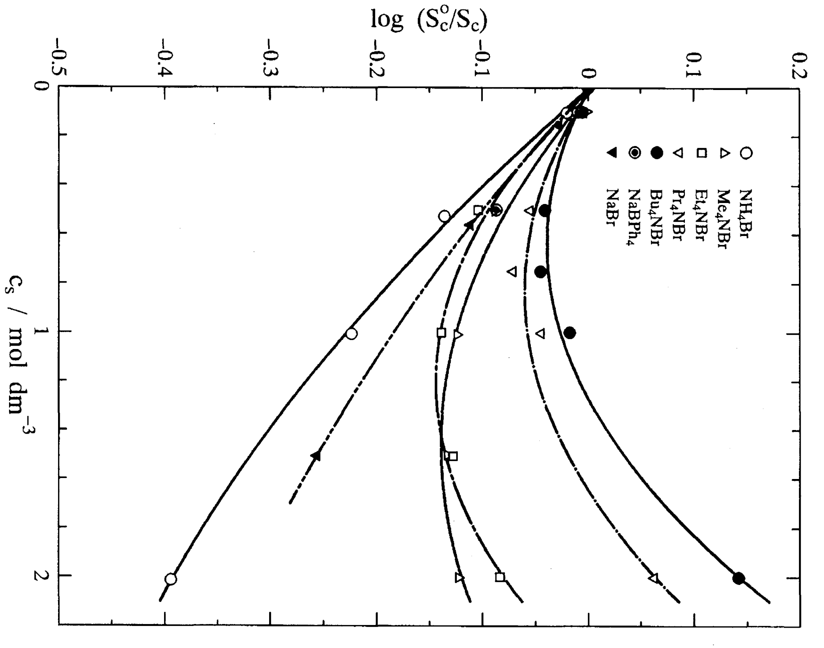

Fig. 2. Salt effect on *mer*-(+)-[Co(L-ala)$_3$] depicted by plotting log (S_c°/S_c) against c_s. The data in aqueous NaBr solutions were taken from Ref. 15.

Table 3. Solubilities (S_m and S_c) of *mer*-(+)-[Co(L-ala)$_3$] in aqueous NH_4Br, Me_4NBr, Et_4NBr, Pr_4NBr, Bu_4NBr, and $NaBPh_4$ Solutions[a)]

T/°C	NH_4Br concentration m_s/mol kg^{-1}				Me_4NBr concentration m_s/mol kg^{-1}				
	0.103	0.541	1.055	2.220	0.099	0.537	1.142	1.821	2.607
	$S_\mathrm{m}/10^{-3}$ mol kg^{-1}				$S_\mathrm{m}/10^{-3}$ mol kg^{-1}				
5	3.35(0.01)	4.54(0.01)	5.60(0.05)	8.41(0.01)	3.20(0.02)	3.95(0.04)	4.29(0.02)	4.35(0.03)	4.21(0.02)
10	3.51(0.01)	4.62(0.01)	5.71(0.02)	8.50(0.03)	3.35(0.01)	4.12(0.03)	4.44(0.02)	4.50(0.02)	4.31(0.02)
15	3.73(0.03)	4.80(0.01)	5.94(0.03)	8.56(0.06)	3.56(0.05)	4.31(0.03)	4.63(0.03)	4.67(0.02)	4.50(0.02)
20	3.94(0.03)	5.03(0.04)	6.13(0.04)	8.72(0.05)	3.76(0.06)	4.53(0.01)	4.86(0.03)	4.87(0.02)	4.70(0.02)
25	4.17(0.01)	5.30(0.03)	6.34(0.03)	8.92(0.02)	3.97(0.02)	4.77(0.03)	5.09(0.03)	5.10(0.02)	4.89(0.02)
30	4.43(0.04)	5.61(0.01)	6.68(0.05)	9.25(0.03)	4.26(0.02)	5.07(0.02)	5.38(0.04)	5.43(0.05)	5.18(0.04)
35	4.78(0.02)	5.98(0.03)	7.12(0.04)	9.67(0.07)	4.56(0.03)	5.41(0.04)	5.76(0.02)	5.75(0.03)	5.51(0.04)
	c_s/mol dm^{-3}				c_s/mol dm^{-3}				
	0.103	0.527	1.005	2.013	0.098	0.504	1.008	1.503	2.002
	$S_\mathrm{c}/10^{-3}$ mol dm^{-3}				$S_\mathrm{c}/10^{-3}$ mol dm^{-3}				
25	4.24(0.02)	5.53(0.03)	6.77(0.03)	10.0(0.1)	4.06(0.02)	4.95(0.03)	5.38(0.03)	5.50(0.02)	5.36(0.02)

T/°C	Et_4NBr concentration m_s/mol kg^{-1}					Pr_4NBr concentration m_s/mol kg^{-1}				
	0.102	0.549	1.211	2.032	3.024	0.105	0.571	0.913	1.313	3.726
	$S_\mathrm{m}/10^{-3}$ mol kg^{-1}					$S_\mathrm{m}/10^{-3}$ mol kg^{-1}				
5	3.24(0.01)	4.03(0.03)	4.34(0.01)	4.11(0.03)	3.57(0.02)	3.20(0.03)	3.51(0.03)	3.47(0.02)	3.17(0.01)	2.33(0.02)
10	3.42(0.01)	4.22(0.01)	4.53(0.01)	4.29(0.03)	3.74(0.04)	3.38(0.03)	3.70(0.01)	3.71(0.03)	3.42(0.01)	2.50(0.04)
15	3.62(0.03)	4.40(0.01)	4.76(0.03)	4.49(0.01)	3.96(0.02)	3.58(0.03)	3.92(0.02)	3.95(0.03)	3.67(0.02)	2.72(0.01)
20	3.84(0.02)	4.69(0.03)	4.99(0.01)	4.75(0.01)	4.16(0.03)	3.84(0.04)	4.18(0.01)	4.26(0.04)	3.95(0.02)	2.99(0.02)
25	4.07(0.01)	4.95(0.01)	5.27(0.02)	5.04(0.04)	4.46(0.06)	4.01(0.03)	4.44(0.05)	4.58(0.04)	4.27(0.02)	3.21(0.02)
30	4.34(0.03)	5.29(0.05)	5.59(0.04)	5.36(0.03)	4.78(0.02)	4.39(0.04)	4.77(0.03)	4.94(0.01)	4.63(0.02)	3.58(0.02)
35	4.64(0.02)	5.62(0.03)	5.98(0.07)	5.75(0.06)	5.14(0.01)	4.70(0.02)	5.12(0.03)	5.33(0.02)	5.01(0.02)	3.93(0.06)
	c_s/mol dm^{-3}					c_s/mol dm^{-3}				
	0.100	0.501	1.000	1.507	2.000	0.102	0.502	0.751	1.002	2.001
	$S_\mathrm{c}/10^{-3}$ mol dm^{-3}					$S_\mathrm{c}/10^{-3}$ mol dm^{-3}				
25	4.16(0.01)	5.14(0.01)	5.57(0.02)	5.43(0.03)	4.91(0.06)	4.09(0.03)	4.59(0.05)	4.77(0.05)	4.49(0.03)	3.50(0.02)

T/°C	Bu_4NBr concentration m_s/mol kg^{-1}					$NaBPh_4$ concentration m_s/mol kg^{-1}	
	0.104	0.590	0.967	1.423	5.009	0.104	0.582
	$S_\mathrm{m}/10^{-3}$ mol kg^{-1}					$S_\mathrm{m}/10^{-3}$ mol kg^{-1}	
5	3.15(0.02)	3.24(0.03)				3.14(0.05)	3.30(0.01)
10	3.33(0.02)	3.47(0.01)	3.40(0.02)			3.28(0.04)	3.57(0.03)
15	3.53(0.03)	3.74(0.02)	3.71(0.02)	3.36(0.02)	2.50(0.02)	3.50(0.02)	3.85(0.02)
20	3.77(0.02)	4.02(0.03)	4.00(0.03)	3.67(0.02)	2.67(0.03)	3.75(0.04)	4.22(0.01)
25	4.02(0.01)	4.31(0.01)	4.33(0.04)	4.03(0.02)	2.81(0.03)	4.06(0.05)	4.73(0.05)
30	4.30(0.03)	4.72(0.05)	4.77(0.02)	4.38(0.03)	3.10(0.03)	4.44(0.02)	5.13(0.04)
35	4.61(0.03)	5.13(0.01)	5.16(0.02)	4.75(0.02)	3.32(0.03)		
40			5.57(0.03)	5.18(0.03)	3.54(0.05)		
	c_s/mol dm^{-3}					c_s/mol dm^{-3}	
	0.101	0.501	0.751	1.000	2.000	0.101	0.500
	$S_\mathrm{c}/10^{-3}$ mol dm^{-3}					$S_\mathrm{c}/10^{-3}$ mol dm^{-3}	
25	4.10(0.01)	4.45(0.01)	4.49(0.04)	4.21(0.02)	2.92(0.04)	4.14(0.05)	4.94(0.05)

a) Errors defined as 95% confidence levels are given in parentheses.

also displayed.

In all the cases, the log ($S_\mathrm{c}^\circ/S_\mathrm{c}$) values are negative up to c_s of 1 mol dm^{-3} (salting-in effect). While the salting-in effect of NH_4Br and NaBr increases monotonously with an increase in c_s, the curves illustrating the effect of tetraalkylammonium bromides pass through a minimum. The salting-in effect in the low c_s region increases in the order of $Bu_4NBr < Pr_4NBr < Me_4NBr < Et_4NBr \approx NaBPh_4 < NaBr < NH_4Br$.

Since these log ($S_\mathrm{c}^\circ/S_\mathrm{c}$) values are connected with the standard free energy of transfer ($\Delta G_\mathrm{tr}^\circ$) from water to the aqueous salt solutions for *mer*-(+)-[Co(L-ala)$_3$], the salting-in effect should be discussed from the standpoint of a contribution of enthalpy and entropy factors. Thus, the standard enthalpy ($\Delta H_\mathrm{tr}^\circ$) and entropy of transfer ($\Delta S_\mathrm{tr}^\circ$) from water to the aqueous salt solutions for *mer*-(+)-[Co(L-ala)$_3$] was calculated by

$$\Delta Y_\mathrm{tr}^\circ = \Delta Y_\mathrm{s}^\circ(\mathrm{salt}) - \Delta Y_\mathrm{s}^\circ(\mathrm{water}), \qquad (1)$$

where Y denotes enthalpy or entropy and $\Delta Y_\mathrm{s}^\circ$(salt) describes

ΔH_s° or ΔS_s° of *mer*-(+)-[Co(L-ala)$_3$] in the aqueous salt solutions estimated from the temperature dependence of $\ln S_m$.

The resulting values for ΔH_{tr}° are plotted against $T\Delta S_{tr}^\circ$ in Fig. 3. Figure 3 indicates that the contribution of ΔH_{tr}° and $T\Delta S_{tr}^\circ$ to the salting-in effect may be classified into two categories by distinguishable characteristics. The first group is composed of NaBr and NH_4Br. In this group, both ΔH_{tr}° and $T\Delta S_{tr}^\circ$ are negative, and decrease with increasing m_s (see Fig. 3). As shown by the broken line in Fig. 3, a linear correlation between ΔH_{tr}° and $T\Delta S_{tr}^\circ$ is found and expressed by

$$\Delta H_{tr}^\circ = 1.71 T\Delta S_{tr}^\circ \quad (\gamma = 0.9801), \tag{2}$$

where γ is the correlation coefficient. Equation 2 is settled by applying the least-squares analysis not only to the data for NaBr and NH_4Br but to the data for $NaNO_3$, NaCl, and NaI reported in the preceding investigation,[15] and indicates that the salting-in effect of these salts is brought about by the decrease in ΔH_{tr}°. These findings suggest that the salting-in effect of NaBr, NH_4Br, $NaNO_3$, NaCl, and NaI on *mer*-(+)-[Co(L-ala)$_3$] has a common origin, which seems to be a hydrophilic interaction such as ion–dipole or hydrogen bond interactions between a polar group (for example the carbonyl group) of *mer*-(+)-[Co(L-ala)$_3$] and the surroundings. An attempt to clarify this origin is intended.

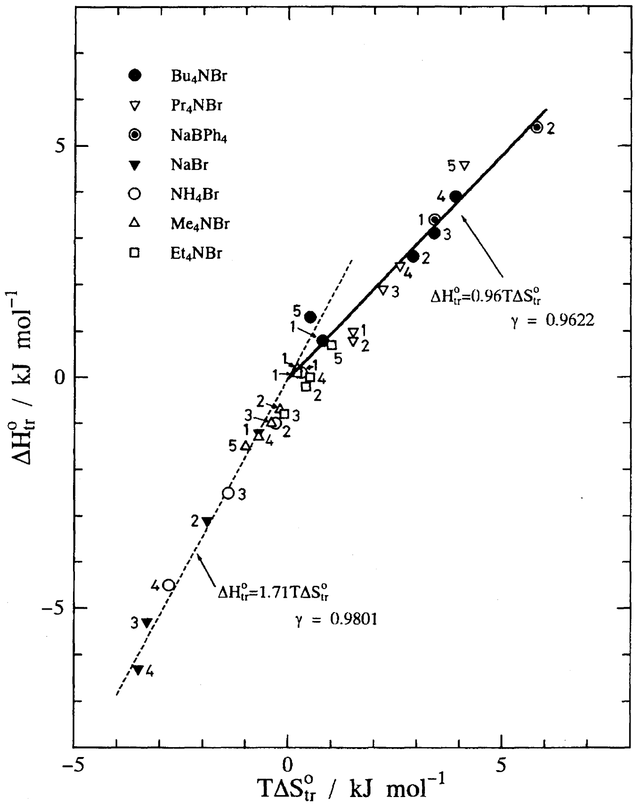

Fig. 3. Correlation between ΔH_{tr}° and $T\Delta S_{tr}^\circ$ for the transfer process of *mer*-(+)-[Co(L-ala)$_3$] from water to aqueous salt solutions. The values of ΔH_{tr}° and $T\Delta S_{tr}^\circ$ for the transfer to NaBr solutions were calculated from the data reported in Ref. 15. The number given beside each mark represents increasing sequence of salt concentration m_s. Each m_s value is given in Table 3.

The second group is composed of Pr_4NBr, Bu_4NBr, and $NaBPh_4$, which result in positive ΔH_{tr}° and $T\Delta S_{tr}^\circ$. The linear correlation between ΔH_{tr}° and $T\Delta S_{tr}^\circ$ (solid line in Fig. 3) presented by

$$\Delta H_{tr}^\circ = 0.96 T\Delta S_{tr}^\circ \quad (\gamma = 0.9622), \tag{3}$$

shows that the salting-in effects of these salts are driven by an increase in $T\Delta S_{tr}^\circ$. A comparison of Eq. 3 with Eq. 2 can present a reasonable explanation for the finding that the salting-in effect of Pr_4NBr, Bu_4NBr, and $NaBPh_4$ is smaller than the salting-in effect of NaBr and NH_4Br (see Fig. 2). Since the slope of the compensation line between ΔH_{tr}° and $T\Delta S_{tr}^\circ$ for the salting-in effect of Pr_4NBr, Bu_4NBr, and $NaBPh_4$ is nearly unitary, the free energy change becomes extremely small.

It is generally accepted that Pr_4N^+, Bu_4N^+, and BPh_4^- ions increase the three-dimensional network structure of water.[26] The idea that hydrophobic interaction is caused by a decrease in the hydration sphere due to attachment of hydrophobic molecules can explain positive enthalpy and entropy changes accompanying the hydrophobic interaction, that is, a decrease in the structured water molecules due to the hydrophobic interaction results in the positive enthalpy and entropy changes.[27]

Thus, the positive ΔH_{tr}° and ΔS_{tr}° in the second group may be regarded as an indication of the hydrophobic interaction between *mer*-(+)-[Co(L-ala)$_3$] and Pr_4N^+, Bu_4N^+, or BPh_4^- ions. The fact that the data for $NaBPh_4$ lie on the same straight line as the data for Pr_4NBr and Bu_4NBr suggests that the positive and negative charges of Pr_4N^+, Bu_4N^+, and BPh_4^- do not affect the hydrophobic interaction. The magnitude of ΔH_{tr}° and $T\Delta S_{tr}^\circ$ for the transfer to the salt solutions with similar m_s (for example, see the points numbered as 2 in Fig. 3) increases in the order of $Pr_4NBr < Bu_4NBr < NaBPh_4$. This result suggests that the increase of the water structure increases in the order of $Pr_4N^+ < Bu_4N^+ < BPh_4^-$. Marcus has claimed the order of $BPh_4^- < Pr_4N^+ < Bu_4N^+$.[26]

Definitive classification of Me_4NBr and Et_4NBr into either group seems to be difficult. The negative ΔH_{tr}° and $T\Delta S_{tr}^\circ$ for these salts agree with the feature in the first group. But the occurrence of the minimum in the salting-in effect profile (see Fig. 2) resembles the salting-in behavior of Pr_4NBr and Bu_4NBr. It has been reported that Me_4N^+ ion has a breaking effect on the water structure and that Et_4N^+ ion results in a borderline effect between the structure breaking and making effect.[26,28] These results on the effects of Me_4NBr and Et_4NBr on the solubility of *mer*-(+)-[Co(L-ala)$_3$] seem to be consistent with the above-mentioned effect of these salts on the water structure.

Effects of Bu_4NBr on the Solubilities of Various *mer*-(+)-[Co(L-aa)$_3$]. As discussed in the preceding section, Bu_4N^+ ion brings about the hydrophobic interaction with *mer*-(+)-[Co(L-ala)$_3$]. To estimate the hydrophobicity of the side chains of some amino acids on the basis of this phenomenon, the solubilities of *mer*-[Co(gly)$_3$], *mer*-(+)-[Co(L-ser)$_3$], *mer*-(−+)-[Co(DL-aba)$_3$], *mer*-(−+)-[Co(DL-nval)$_3$], *mer*-(+)-[Co(L-val)$_3$], and *mer*-(+)-[Co(L-leu)$_3$] in aqueous Bu_4NBr solutions were measured. These solubility data are tabulated in Table 4. The effects of Bu_4NBr are depicted in Fig. 4 by plot-

Table 4. Solubilities (S_m and S_c) of *mer*-[Co(gly)$_3$], *mer*-(+)-[Co(L-ser)$_3$], *mer*-(−+)-[Co(DL-aba)$_3$], *mer*-(−+)-[Co(DL-nval)$_3$], *mer*-(+)-[Co(L-val)$_3$], and *mer*-(+)-[Co(L-leu)$_3$] in Aqueous Bu_4NBr Solutions[a)]

T/°C	*mer*-[Co(gly)$_3$]					*mer*-(+)-[Co(L-val)$_3$]		
	m_s/mol kg^{-1}					m_s/mol kg^{-1}		
	0.158	0.590	0.969	1.428	4.993	0.214	0.595	0.969
	$S_m/10^{-2}$ mol kg^{-1}					$S_m/10^{-1}$ mol kg^{-1}		
5	1.37(0.01)	1.32(0.01)				1.65(0.01)	1.67(0.02)	
10	1.68(0.01)	1.65(0.01)	1.55(0.01)	1.49(0.01)	1.20(0.01)	1.54(0.01)	1.63(0.01)	1.57(0.01)
15	2.11(0.02)	2.05(0.01)	1.92(0.02)	1.86(0.01)	1.37(0.01)	1.38(0.01)	1.55(0.01)	1.53(0.01)
20	2.62(0.01)	2.54(0.01)	2.39(0.04)	2.27(0.01)	1.56(0.01)	1.31(0.01)	1.43(0.02)	1.50(0.01)
25	3.24(0.01)	3.13(0.01)	2.87(0.04)	2.77(0.02)	1.80(0.01)	1.23(0.01)	1.39(0.01)	1.50(0.01)
30	3.94(0.02)	3.86(0.02)	3.38(0.02)	3.35(0.03)	2.07(0.02)	1.12(0.01)	1.42(0.01)	1.54(0.02)
35	4.83(0.02)	4.68(0.01)		4.06(0.01)		1.08(0.01)	1.42(0.01)	1.61(0.01)
40				4.79(0.03)		1.08(0.01)	1.44(0.02)	1.69(0.02)
	c_s/mol dm^{-3}					c_s/mol dm^{-3}		
	0.150	0.500	0.750	1.000	1.995	0.200	0.504	0.751
	$S_c/10^{-2}$ mol dm^{-3}					$S_c/10^{-1}$ mol dm^{-3}		
25	3.32(0.01)	3.24(0.01)	2.99(0.04)	2.90(0.02)	1.90(0.02)	1.24(0.01)	1.41(0.02)	1.52(0.01)
T/°C	*mer*-(+)-[Co(L-ser)$_3$]				*mer*-(−+)-[Co(DL-aba)$_3$]			
	m_s/mol kg^{-1}				m_s/mol kg^{-1}			
	0.214	0.591	0.966	1.433	0.159	0.590	0.972	1.430
	$S_m/10^{-2}$ mol kg^{-1}				$S_m/10^{-2}$ mol kg^{-1}			
5	0.417(0.005)	0.379(0.004)			1.04(0.01)	1.19(0.01)		
10	0.520(0.004)	0.484(0.006)	0.487(0.002)	0.386(0.001)	1.12(0.01)	1.22(0.01)	1.18(0.01)	1.15(0.01)
15	0.676(0.004)	0.619(0.011)	0.625(0.006)	0.501(0.004)	1.26(0.01)	1.40(0.01)	1.36(0.01)	1.35(0.01)
20	0.858(0.012)	0.815(0.009)	0.802(0.005)	0.652(0.004)	1.44(0.01)	1.64(0.01)	1.64(0.01)	1.64(0.02)
25	1.11(0.01)	1.06(0.01)	1.04(0.01)	0.859(0.004)	1.67(0.01)	1.94(0.01)	2.00(0.02)	2.03(0.03)
30	1.43(0.01)	1.20(0.01)	1.12(0.01)	0.944(0.010)	2.02(0.01)	2.37(0.02)	2.45(0.01)	2.50(0.04)
35	1.50(0.01)	1.36(0.01)	1.24(0.01)	1.06(0.01)	2.40(0.02)	2.84(0.02)	2.99 (0.02)	3.21(0.03)
40	1.67(0.01)	1.52(0.02)	1.38(0.02)	1.18(0.01)	2.84(0.02)	3.45(0.03)	3.72(0.02)	3.93(0.04)
	c_s/mol dm^{-3}				c_s/mol dm^{-3}			
	0.201	0.502	0.750	1.005	0.151	0.500	0.752	1.001
	$S_c/10^{-2}$ mol dm^{-3}				$S_c/10^{-2}$ mol dm^{-3}			
25	1.14(0.01)	1.10(0.01)	1.09(0.01)	0.901(0.001)	1.72(0.01)	2.00(0.01)	2.09(0.02)	2.13(0.03)
T/°C	*mer*-(−+)-[Co(DL-nval)$_3$]				*mer*-(+)-[Co(L-leu)$_3$]			
	m_s/mol kg^{-1}				m_s/mol kg^{-1}			
	0.164	0.590	0.969	1.429	0.589	0.969	1.435	2.124
	$S_m/10^{-2}$ mol kg^{-1}				$S_m/10^{-3}$ mol kg^{-1}			
5	2.49(0.01)	3.31(0.03)			0.749(0.008)			
10	2.49(0.02)	3.33(0.01)	3.85(0.03)	3.72(0.04)	0.727(0.008)	0.850(0.008)	1.10(0.01)	2.07(0.02)
15	2.46(0.01)	3.34(0.03)	3.78(0.02)	3.90(0.03)	0.715(0.015)	0.869(0.015)	1.19(0.01)	2.18(0.02)
20	2.48(0.02)	3.27(0.04)	3.82(0.01)	4.06(0.03)	0.723(0.012)	0.929(0.013)	1.34(0.01)	2.55(0.01)
25	2.49(0.02)	3.35(0.03)	3.89(0.04)	4.32(0.04)	0.741(0.005)	1.02(0.01)	1.56(0.02)	2.96(0.03)
30	2.50(0.01)	3.37(0.05)	4.03(0.03)	4.73(0.02)	0.789(0.005)	1.16(0.01)	1.82(0.01)	3.54(0.06)
35	2.53(0.02)	3.47(0.03)	4.28(0.04)	5.30(0.05)	0.873(0.011)	1.32(0.01)	2.18(0.03)	4.17(0.03)
40	2.59(0.02)	3.65(0.04)	4.74(0.10)	6.35(0.15)	0.965(0.010)	1.52(0.03)	2.60(0.05)	
	c_s/mol dm^{-3}				c_s/mol dm^{-3}			
	0.156	0.500	0.751	1.000	0.5000	0.751	1.005	1.301
	$S_c/10^{-2}$ mol dm^{-3}				$S_c/10^{-3}$ mol dm^{-3}			
25	2.55(0.02)	3.45(0.02)	4.03(0.04)	4.56(0.03)	0.759(0.007)	1.06(0.01)	1.62(0.02)	3.13(0.04)

a) Errors defined as 95% confidence levels are given in parentheses.

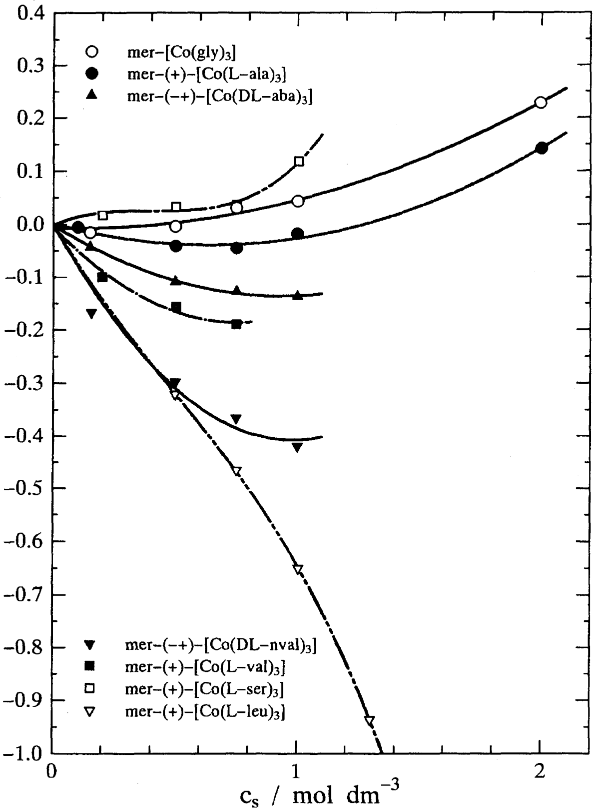

Fig. 4. Effect of Bu_4NBr on various *mer*-[Co(aa)$_3$] depicted by plotting log (S_c°/S_c) against c_s.

ting log (S_c°/S_c) against c_s. The salting-in effect of Bu_4NBr increases in the order of *mer*-(+)-[Co(L-ala)$_3$] < *mer*-(-+)-[Co(DL-aba)$_3$] < *mer*-(+)-[Co(L-val)$_3$] < *mer*-(−+)-[Co(DL-nval)$_3$] < *mer*-(+)-[Co(L-leu)$_3$]. The addition of Bu_4NBr to *mer*-[Co(gly)$_3$] and *mer*-(+)-[Co(L-ser)$_3$] solutions has a slight salting-out effect.

As shown in Fig. 5, when ΔH_{tr}° was plotted against $T\Delta S_{tr}^\circ$ for the transfer process of these chelates from water to aqueous Bu_4NBr solutions, a single correlation line through all the data, including the data for *mer*-(+)-[Co(L-ala)$_3$], was obtained. This finding indicates that the effect of Bu_4NBr on the solubilities of all the chelates studied in this investigation has the same origin (hydrophobic interaction) as the effect on *mer*-(+)-[Co(L-ala)$_3$] discussed in the preceding section. The correlation is expressed by

$$\Delta H_{tr}^\circ = 0.87 T\Delta S_{tr}^\circ \quad (\gamma = 0.9985). \tag{4}$$

For *mer*-(+)-[Co(L-ala)$_3$], *mer*-(−+)-[Co(DL-aba)$_3$], *mer*-(−+)-[Co(DL-nval)$_3$], *mer*-(+)-[Co(L-val)$_3$], and *mer*-(+)-[Co(L-leu)$_3$], both ΔH_{tr}° and $T\Delta S_{tr}^\circ$ are positive and increase with increasing m_s (see Fig. 5). The salting-in effect is driven by the increase in $T\Delta S_{tr}^\circ$. On the other hand, for *mer*-[Co(gly)$_3$] and *mer*-(+)-[Co(L-ser)$_3$] both ΔH_{tr}° and $T\Delta S_{tr}^\circ$ generally decrease with increasing m_s (see Fig. 5). The decrease in $T\Delta S_{tr}^\circ$ results in the salting-out effect.

The variation of log (S_c°/S_c) with c_s shown in Fig. 4 is liable to be regarded as an indication of the strength of the hydrophobic interaction. But the term of log (S_c°/S_c) is related to ΔG_{tr}°. As discussed in the preceding section, it is more reasonable to use ΔH_{tr}° or $T\Delta S_{tr}^\circ$ rather than ΔG_{tr}° to estimate the hydrophobicity of side chains of amino acids.

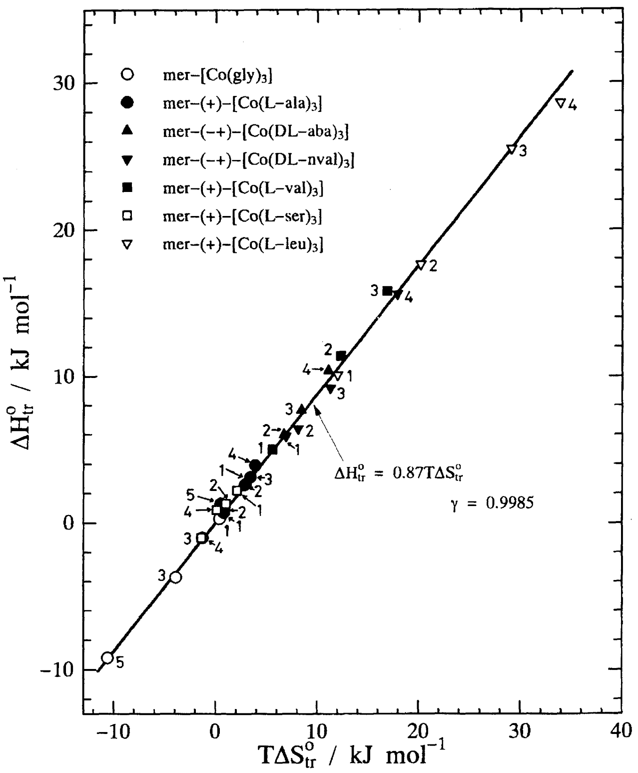

Fig. 5. Compensation relation between ΔH_{tr}° and $T\Delta S_{tr}^\circ$ for the transfer process of various *mer*-[Co(aa)$_3$] from water to aqueous Bu_4NBr solutions. The number given beside each mark represents increasing sequence of Bu_4NBr concentration m_s. Each m_s value is given in Table 4.

Thus, ΔH_{tr}° or $T\Delta S_{tr}^\circ$ for the transfer of *mer*-(+)-[Co(L-aa)$_3$] from water to 0.97 mol kg^{-1} Bu_4NBr solution is plotted against carbon atom numbers in side chains of the corresponding amino acids in Fig. 6. Both ΔH_{tr}° and $T\Delta S_{tr}^\circ$ increase with the increasing carbon atom numbers. This implies that the hydrophobic interaction of *mer*-(+)-[Co(L-aa)$_3$] with Bu_4N^+ ion increases with increasing side chain length of amino acid and that the hydrophobicity increases in the order of glyH < serH < alaH < abaH < nvalH < valH < leuH.

The order of glyH < alaH < valH < leuH is consistent with the order based on several criteria for the hydrophobicity.[29] This confirms the validity of the present approach using [Co(aa)$_3$] as the model compound for amino acid residues of proteins. While the effect of alkyl chain branching on the hydrophobicity of aliphatic compounds seems not to give a concordant conclusion,[30] a comparison of the ΔH_{tr}° and $T\Delta S_{tr}^\circ$ values for *mer*-(+)-[Co(L-val)$_3$] with the ΔH_{tr}° and $T\Delta S_{tr}^\circ$ values for *mer*-(−+)-[Co(DL-nval)$_3$] suggests that the chain branching increases the hydrophobicity. Introduction of a hydrophilic hydroxyl group into alaH may be expected to reduce the hydrophobicity. The hydrophobicity order in this study is consistent with this expectation. Nozaki and Tanford have reported that the amino acids with aromatic rings such as tryptophan and phenylalanine have large hydrophobicity.[21]

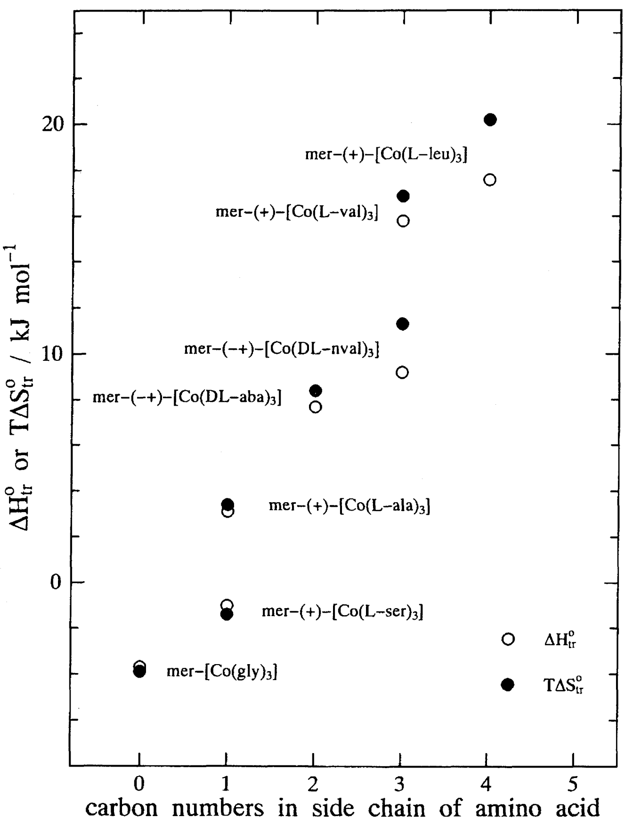

Fig. 6. Plot of ΔH°_{tr} or $T\Delta S^\circ_{tr}$ for *mer*-[Co(aa)$_3$] against carbon atom numbers in side chains of amino acids. The values of ΔH°_{tr} and $T\Delta S^\circ_{tr}$ correspond to the transfer from water to 0.97 mol kg^{-1} Bu$_4$NBr solution.

Synthesis of [Co(aa)$_3$] using these amino acids was also tried in this study but the attempt was unsuccessful. A synthetic effort would be developed in the near future.

While the correlation between ΔH°_{tr} or $T\Delta S^\circ_{tr}$ and the carbon atom numbers shown in Fig. 6 is too rough to estimate an increment of ΔH°_{tr} or $T\Delta S^\circ_{tr}$ per methylene group, the hydrophobic interaction of [Co(L-aa)$_3$] with Bu$_4$N$^+$ ion can provide useful information for the hydrophobicity of amino acids. Thus, it would be interesting to examine some properties of [Co(aa)$_3$] in Bu$_4$NBr solution such as volumetric property and viscosity, and to compare with the results so far reported for the amino acids themselves.

References

1) D. P. Kharakoz, *Biophys. Chem.*, **34**, 115 (1989).

2) K. B. Belibagl and E. Ayranc, *J. Solution Chem.*, **19**, 867 (1990).

3) D. P. Kharakoz, *J. Phys. Chem.*, **95**, 5634 (1991).

4) A. W. Hakin, M. M. Duke, S. A. Klassen, R. M. McKay, and K. E. Preuss, *Can. J. Chem.*, **72**, 362 (1994).

5) M. M. Duke, A. W. Hakin, R. M. McKay, and K. E. Preuss, *Can. J. Chem.*, **72**, 1489 (1994).

6) Z. Yan, J. Wang, H. Zheng, and D. Liu, *J. Solution Chem.*, **27**, 473 (1998).

7) G. R. Hedwig and H. Høiland, *J. Solution Chem.*, **20**, 1113 (1991).

8) O. V. Kulikov, A. Zielenkiewicz, W. Zielenkiewicz, V. G. Badelin, and G. A. Krestov, *J. Solution Chem.*, **22**, 59 (1993).

9) A. W. Hakin, M. M. Duke, L. L. Groft, J. L. Marty, and M. L. Rushfeldt, *Can. J. Chem.*, **73**, 725 (1995).

10) G. R. Hedwig, J. D. Hastie, and H. Høiland, *J. Solution Chem.*, **25**, 615 (1996).

11) M. Kikuchi, M. Sakurai, and K. Nitta, *J. Chem. Eng. Data*, **41**, 1439 (1996).

12) M. Mizuguchi, M. Sakurai, and K. Nitta, *J. Solution Chem.*, **26**, 579 (1997).

13) a) Y. Yoshimura, *Inorg. Chim. Acta*, **207**, 65 (1993); b) Y. Yoshimura, *Bull. Chem. Soc. Jpn.*, **68**, 2305 (1995).

14) Y. Yoshimura, *Bull. Chem. Soc. Jpn.*, **69**, 2565 (1996).

15) Y. Yoshimura, *Can. J. Chem.*, **76**, 71 (1998).

16) R. Tenne and A. Ben-Naim, *J. Phys. Chem.*, **80**, 1120 (1976).

17) E. Iwamoto, Y. Tanaka, H. Kimura, and Y. Yamamoto, *J. Solution Chem.*, **9**, 841 (1980).

18) a) C-H. Chen, *J. Phys. Chem.*, **84**, 2050 (1980); b) C-H. Chen, *J. Phys. Chem.*, **85**, 603 (1981).

19) A. Delville, P. Laszlo, and A. Stockis, *J. Am. Chem. Soc.*, **103**, 5991 (1981).

20) D. Eisenberg, R. M. Weiss, T. C. Terwilliger, and W. Wilcox, *Faraday Symp. Chem. Soc.*, **17**, 109 (1982)

21) .Y. Nozaki and C. Tanford, *J. Biol. Chem.*, **246**, 2211 (1971).

22) B. E. Douglas and S. Yamada, *Inorg. Chem.*, **4**, 1561 (1965).

23) R. G. Denning and T. S. Piper, *Inorg. Chem.*, **5**, 1056 (1966).

24) R. D. Gillard and N. C. Payne, *J. Chem. Soc. A*, **1969**, 1197.

25) Y. Yoshimura, *Can. J. Chem.*, **67**, 2108 (1989).

26) Y. Marcus, *J. Solution Chem.*, **23**, 831 (1994).

27) A. Ben-Naim, "Hydrophobic Interaction," Plenum Press, New York (1980).

28) P. R. Philip and C. Jolicoeur, *J. Phys. Chem.*, **77**, 3071 (1973).

29) D. Hecht, L. Tadesse, and L. Walters, *J. Am. Chem. Soc.*, **115**, 3336 (1993).

30) J. C. Ahluwalia, *J. Indian Chem. Soc.*, **56**, 115 (1979).